Polyacrylamide strengthened mixed-charge hydrogels and their applications in resistance to protein adsorption and algae attachment

Daoyi Jiang, Zhixiong Liu,* Xiaoyan He, Jin Han* and Xuedong Wu

Mixed-charge polymer hydrogels were successfully prepared by copolymerization of different ratios of [2-(meth-acryloyloxy) ethyl] trimethylammonium (TMA) and 3-sulfopropyl methacrylate (SA). Then, a second polyacrylamide (PAAM) network was incorporated into the pre-prepared hydrogel to form a double network (DN) hydrogel. The compositions of these DN hydrogels were characterized by Fourier transform infrared spectroscopy (FTIR) and X-ray photoelectron spectroscopy (XPS). Rheological and compressive measurements confirmed that the mechanical performances of the DN hydrogels were significantly improved by incorporation of a second PAAM network, compared with the according single network (SN) hydrogels. The amount of protein absorbed on the DN hydrogel surface was related to the ratio of TMA/SA and the ionic strength. The DN hydrogel with equal amount of TMA and SA exhibited better protein resistance. In addition, *Phaeodactylum tricornutum* and *Chlorella* were chosen for the anti-algae assay. The results displayed that the negatively charged hydrogels showed better anti-algae fouling performance than the positively charged and the neutral DN hydrogels. These DN hydrogels have promising applications in marine antifouling coating and interfaces of biomaterials.

Introduction

Undesirable accumulation of microorganisms, plants and marine animals on submerged surfaces is a serious problem for marine activities and industries.[1–4] Antifouling (AF) coatings have been developed to prevent the settlement of fouling organisms. Traditional biocidal coatings containing heavy metals are detrimental to non-targeted fouling organism and ecologically harmful.[5–7] Many efforts have been devoted to develop environmentally friendly anti-biofouling systems including self-polishing resins, amphiphilic nanostructured coatings,[8–12] low surface energy elastomers,[13,14] bioinspired engineered topographies[15,16] enzymes,[17,18] antifoulants made of natural products[19–22] and hydrogels.[23–25]

Zwitterionic polymers, in which both cationic and anionic groups are on the same monomer, have been reported to be highly resistant to nonspecific protein adsorption. Zwitterionic hydrogels are considered one promising environment-friendly antifouling coatings since these exhibit superhydrophilic properties and strong resistances to protein adsorption, cell attachment and bacterial adhesion.[26–29] Jiang *et al.* prepared zwitterionic hydrogels such as poly(sulfobetaine methacrylate) (PSBMA) and poly(carboxybetaine methacrylate) (PCBMA) which show excellent resistance to BAEC adhesion *in vitro*.[27] Recently, a new class of copolymer hydrogels based on the PSBMA and starch were prepared and exhibited good anti-biofouling efficiency and biocompatibility.[28] However, some zwitterionic monomers like 2-methacryloyloxyethyl phosphorylcholine (MPC) are harder to synthesize.[30] Mixed-charge polymers containing equal amount of positive and negative charged regions are equivalent to zwitterionic materials and also highly resistant to nonspecific protein adsorption.[31] Compared with zwitterionic monomers, the monomers used to synthesize mixed-charge polymers are much more readily available. Moreover, a wide spectrum of new nonfouling mixed-charge hydrogels can be designed and prepared by simple tuning the mixed charges.[32,33] In reality, after the absorption of water, the hydrogels especially zwitterionic hydrogel and mixed-charge hydrogel are easily damaged by an external force and not strongly adhesive to the surfaces, which greatly limits their use in marine antifouling.

More recently, various strategies and concepts developed to make tough hydrogels include interpenetrating and double networks,[34] slide ring polymer hydrogels,[35] topological hydrogels,[36] ionically cross-linked copolymers,[37] nanocomposite polymer hydrogels,[38–41] self-assembled microcomposite hydrogels *etc.* Among them, incorporating relatively high molecular mass soft polymer network into a swollen heterogeneous polyelectrolyte network to make a double-network (DN) hydrogel is one of most effective approaches to improve the mechanical strength of the hydrogel. Gong's group developed double network hydrogels from polyzwitterions using DN concept and

Key Laboratory of Marine Materials and Related Technologies, Zhejiang Key Laboratory of Marine Materials and Protective Technologies, Ningbo Institute of Materials Technology and Engineering, Chinese Academy of Sciences, Ningbo, 315201, P. R. China. E-mail: liuzhixiong@nimte.ac.cn

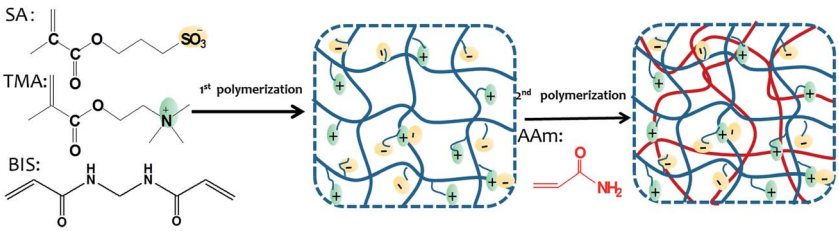

Scheme 1 Schematic illustration of the synthetic route for the DN hydrogels.

the prepared double network hydrogels showed much improved mechanical strength.[42]

Herein, we proposed to strengthen the mixed-charge hydrogel using DN principle and prepared a series of double-network hydrogels with excellent antifouling properties. The antifouling DN hydrogels were made on the basis of the following considerations. Firstly, a series of polyelectrolyte hydrogels with different mixed charges could be synthesized easily and the mixed-charge hydrogels have been widely used to develop antifouling coatings. Secondly, the mechanical strength of the polyelectrolyte hydrogel could be much improved by preparing a DN hydrogel. The DN hydrogels were prepared by a two-step sequential free-radical polymerization (Scheme 1). The first polyelectrolyte hydrogels were obtained by copolymerization of different ratio of [2-(meth-acryloyloxy)ethyl] trimethylammonium (TMA) and 3-sulfopropyl methacrylate (SA). Then, the polyelectrolyte hydrogels were immersed in an aqueous solution of acrylamide (AAM) monomers with a low ratio of bis-acrylamide (BIS) cross-linking agent and a second polymerization in the network was conducted. The mechanical properties of the single network (SN) hydrogels and the DN hydrogels were measured *via* rheological experiments. The protein absorption and the algae settlement behaviors of the DN hydrogels were presented. The DN hydrogels have promising potential applications in marine antifouling coating and interfaces of biomaterials.

Experimental

Materials

Bis-acrylamide (BIS) was purchased from J&K chemical (Beijing, China). [2-(Meth-acryloyloxy)ethyl]trimethylammonium (TMA, 80 wt% aqueous solution) and 3-sulfopropyl methacrylate (SA) were obtained from Sigma-Aldrich. Water-soluble photo-initiator α-ketoglutaric acid (KA), acrylamide (AAM) (AR, 99.0%) and lysozyme from chicken egg white (LYZ, ≥5000 units per mg dry weight) were purchased from Aladdin (Shanghai, China). Albumin from bovine serum (BSA, 98%) was purchased from Sinopharm Chemical Reagent Co. Ltd (Shanghai, China). Deionized water was obtained by using a Millipore water system, with a minimum resistivity of 18.0 MΩ cm. BCA protein assay kit (containing Solution A and Solution B) was purchased from Ningbo Hangjing Biological Technology Co. Ltd. Other reagents were used as received. Artificial seawater is composed of NaCl (26.73 g L^{-1}), $MgCl_2$ (2.26 g L^{-1}), $MgSO_4$ (3.25 g L^{-1}), $CaCl_2$ (1.15 g L^{-1}), $NaHCO_3$ (0.20 g L^{-1}), KCl (0.72 g L^{-1}), NaBr (0.058 g L^{-1}), H_3BO_3 (0.058 g L^{-1}), Na_2SiO_3 (0.0024 g L^{-1}), H_3PO_4 (0.0020 g L^{-1}), Al_2Cl_6 (0.013 g L^{-1}), NH_3 (0.0020 g L^{-1}) and $LiNO_3$ (0.0013 g L^{-1}).

Preparation of the DN hydrogels

The DN hydrogel sheets were synthesized by a two-step free radical polymerization. The first polyelectrolyte hydrogels were prepared by copolymerization of varying ratio of TMA and SA. The aqueous solutions containing TMA, SA, BIS crosslinking agent and KA photo-initiator (Table 1) were injected into plate-to-plate or plastic syringe molds and irradiated with a UV lamp (365 nm, 36 W) for 8 h. These prepared hydrogels were immersed in water to remove unreacted monomers for 2 days. The first prepared hydrogels were then transferred into a 20 wt% AAM aqueous solution (0.14 mol AAM, 4.2 mmol BIS, 0.34 mmol KA, 40 mL water). The DN hydrogels were synthesized by UV irradiation of the immersed hydrogels for 10 h. These DN hydrogels were then soaked in water for a week to remove unreacted monomers. The SN and DN hydrogels were referred to SN-*x*-*y* and DN-*x*-*y* respectively, where *x* and *y* represent the feed molar ratio of TMA and SA.

Chemical characterization of the hydrogels and the swelling behavior

FTIR were recorded using a NICOLET 6700 spectrometer. The freeze-dried hydrogels were ground into powders, blended with

Table 1 The feed ratios of the SN hydrogels

Hydrogel no.	TMA/mmol	SA/mmol	Deionized water/mL	KA/mmol	BIS/mmol
SN-0-10	0	12.83	10.00	0.14	1.4
SN-3-7	3.85	8.97	9.80	0.14	1.4
SN-5-5	6.43	6.41	9.66	0.14	1.4
SN-7-3	8.97	3.25	9.53	0.14	1.4
SN-10-0	12.83	0	9.33	0.14	1.4

dry spectroscopic grade KBr powders, and pressed into small disks for FTIR measurements. XPS measurements were performed on AXIS UTLTRA DLD. All samples were freeze-dried and pressed into thin slices. In addition, the swelling behaviors of hydrogels were studied by measuring the weight of the swollen hydrogels (W_s) and the freeze-dried hydrogels (W_0). The dried hydrogel samples were cut into the disks and immersed in deionized water or artificial seawater for 48 h. The residual water on the surfaces of the hydrogels was wiped with wet filter paper. The swelling ratio (SR) was calculated according to the equation: $SR = (W_s - W_0)/W_0$.

Rheological measurements

Rheological experiments were performed on a rheometer (Physica MCR-301) to test the mechanical performance. All the hydrogels were rinsed in artificial seawater and cut into small disks of similar size ($\varnothing$ = 25 mm and 0.085–1.5 mm gap). Firstly, the linear viscoelastic region (LVR) could be confirmed by the strain amplitude sweeps (γ = 0.001–10) at a constant angular frequency ($\omega = 1$ rad s^{-1}). Then, the storage (G') and the loss moduli (G'') within the LVR were recorded at a constant strain amplitude (γ = 0.5%) with a frequency from 0.1 to 100 rad s^{-1}. All of the samples were measured at room temperature, and the measurements were repeated three times.

Mechanical measurements

The compressive performances of the SN and DN hydrogels were tested by a tensile-compressive tester (Instron 5567, Instron Co.). Hydrogel samples (12.0 mm diameter cylinder, the height is about 12.0–15.0 mm) were placed on the center of the lower compression plate. Then, the sample was compressed by the upper plate at a velocity of 1.0 mm min^{-1}. Elastic modulus values obtained by calculated the slope compressive stress–strain curves from the initial 1–5% strain.

Protein absorption assay

In order to explore the effect of ionic strength on protein adsorption, all of these DN hydrogels were immersed in the NaCl aqueous solutions of the different concentrations (0, 0.1, 0.2, and 0.4 M) for two days. Then, these pretreated hydrogels were cut into small disks equal to the size of well bottom of 24-well plate and fixed on the bottom of the wells. BSA and LYZ, which have different isoelectric point (PI), were chosen as model proteins to examine the antifouling properties of these DN hydrogels. A 1 mg mL^{-1} protein aqueous solution (500 μL 2 mg mL^{-1} protein aqueous solution and 500 μL NaCl aqueous solutions of different concentrations) was poured into the wells and incubated for 4 h. Then, these hydrogels were rinsed with the NaCl aqueous solution to remove the free protein molecules. Finally, the hydrogels fouled by the proteins were washed with a 1.5 wt% SDS aqueous solution. The protein concentration in the SDS solutions was measured by MicroBCA protein assay reagent kit at 562 nm. The amounts of proteins adsorbed on the surfaces of hydrogels were calculated according to the standard curve.

Algae static assay

Phaeodactylum tricornutum and *Chlorella* settlement assays were carried out as follows. The charged DN hydrogels were cut into the disks and fixed at the bottom of a 24-well plate. 1 mL of artificial seawater was poured into the well and discarded after 24 h. 1 mL of microorganism suspension was then added into each well. The plates were incubated in a biochemical incubator for 1 day and 7 days, respectively. The initial concentrations of *Phaeodactylum tricornutum* and *Chlorella* were $(2.7 \pm 0.3) \times 10^8$ and $(1.7 \pm 0.3) \times 10^8$ cells per mL, respectively. After 1 day and 7 days of incubation, these hydrogels were washed three times with artificial seawater to remove the cells that did not adhere or adhered loosely. The samples were placed in a 2.5 vol% glutaraldehyde solution for 15 min to fix cells on the substrates and then twice washed with seawater. The *Phaeodactylum tricornutum* and *Chlorella* settlements were observed by Dimension 3100v Laser Scanning Confocal Microscope (LSCM) analysis system. The quantitative coverage of the cells on the surfaces of hydrogels was calculated by software ImageJ based on the laser confocal images. The experiment for each sample was repeated three times.

Results and discussion

Characterization of the hydrogels and the swelling behavior

These hydrogels were prepared by a two-step sequential free-radical polymerization. The first network was obtained by copolymerization of TMA and SA. The monomer concentrations played an important role in the gelation process. In the SN-5-5 hydrogel system, the critical monomer concentration of TMA and SA was 0.16 mol L^{-1} and 0.16 mol L^{-1}. The second network of the crosslinked PAAM was further introduced to strengthen the hydrogel systems. Fig. 1 displayed the FTIR spectra of these DN hydrogels. The characteristic peak of C=O stretch of the charged SA and TMA located at 1727 cm^{-1}. The bands at 1039 and 954 cm^{-1} corresponded to the functional groups of SA and TMA, respectively.[43] The strong absorption bands at 3434 and 1665 cm^{-1} were attributed to NH_2 and C=O stretch in the AAM fragment, indicating the successful incorporation of PAAM network into the TMA-*co*-SA network.

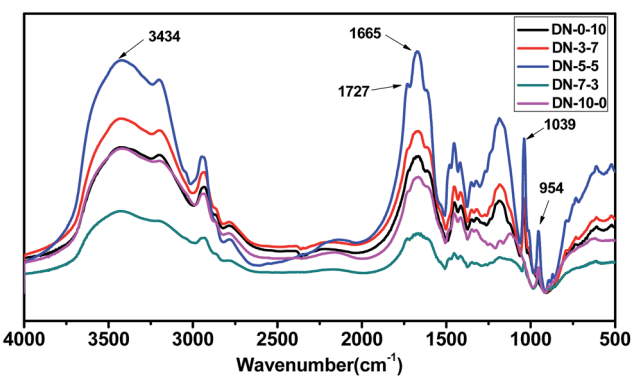

Fig. 1 FTIR spectra of the DN hydrogels with the different ratios of TMA and SA.

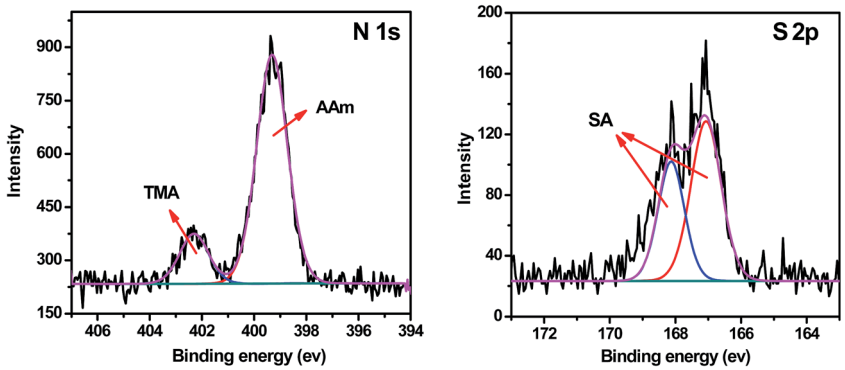

Fig. 2 N1s and S2p XPS spectra of the DN-7-3 hydrogel.

XPS measurements were performed to quantify the hydrogels' compositions. The mole ratio of TMA, SA and AAM in the hydrogels was acquired by investigating N1s and S2p spectra (Fig. 2). Considering the crosslinker BIS was negligible in the gel system, the mole fraction of TMA, SA and AAM can be calculated according to the spectral area ratio of the bands approximately at 399, 402 and 168 eV respectively. Table 2 presented that the mole ratio of the first network to the second one (TMA + SA to AAM) increased initially and then decreased with the mass ratio of TMA to SA monomers, implying that the swelling behavior of the first network in the AAM solution was influenced by the electrostatic interaction of the charged groups in the polyelectrolyte hydrogels. When the ratio of TMA to SA approached 1.0, the sulfonic acid and the quaternary amino groups bound together and restricted the swelling of the hydrogels. Moreover, the concentration of the first network to the second one in the DN-0-10 sample is slightly lower than that in the DN-10-0 hydrogel. The reason might be that the water-binding ability of SA is greater than TMA.

The swelling behavior of the DN hydrogels in deionized water and artificial seawater was showed in Fig. 3. The equilibrium swelling ratio of the hydrogels showed a V-shape as a function of the molar ratio of TMA to SA. The swelling ratio of the DN-5-5 hydrogel is the lowest one in all of the tested DN hydrogels in both deionized and artificial seawater. The explanation is that equal positively and negatively charged groups bound strongly in a SN-5-5 hydrogel and resulted in a poor swelling behavior in the AAM solution. The confined three-dimensional structure of DN-5-5 hydrogel further reduced the intake of water. The ionic strength is also an important factor that affecting the swelling performance of the hydrogels.

Table 2 The calculated compositions of the DN hydrogels by analyzing XPS spectra

Entry	TMA/AAM	TMA/SA	TMA + SA/AAM
DN-0-10	0/1	0/10	1/9.75
DN-3-7	1/21.45	3.36/7	1/7.65
DN-5-5	1/5.59	5.05/5	1/2.81
DN-7-3	1/5.82	6.48/3	1/4.68
DN-10-0	1/7.2	10/0	1/7.2

The equalized swelling ratio of these DN hydrogels in artificial seawater is lower than that in deionized water. The reason may be that sodium and chloride ions, which permeate into the hydrogel system, interact with counterions and weaken the water-binding capacity of the charged groups. In addition, the swelling ratio decreases due to the high ionic osmotic pressure that exerting on the hydrogel system.[44]

Rheological properties of hydrogels

Polyelectrolyte hydrogels are composed of charged three-dimensional network. They are brittle and lack of flexibility.[45] The mechanical strength and toughness performances of the pre-prepared charged hydrogels were enhanced greatly with incorporation of a second PAAM polymer network. Rheological measurements were performed to examine the mechanical properties of the SN hydrogels and the DN hydrogels. Fig. 4 showed the G' and the G'' of the SN and the DN hydrogels as a function of frequency. Strain amplitude sweeps were performed for each sample to determine the linear viscoelastic region (data not shown). Frequency sweeps were then performed at 0.5% strain within the LVR. The G' at the employed frequencies were higher than the G'', which indicated that these hydrogels are highly elastic. With reference to Fig. 4, both the G' and the G'' of the DN gels were much greater than those of the corresponding SN gels, confirming that the mechanical properties were improved significantly. Besides, the G' of the DN gels

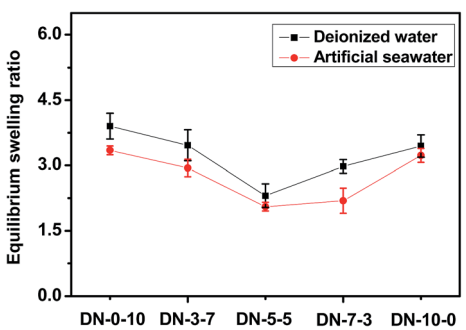

Fig. 3 The swelling behavior of the DN hydrogels in deionized water and artificial seawater.

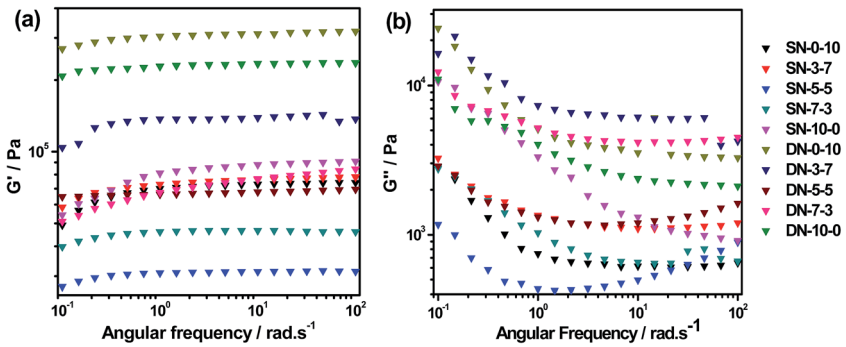

Fig. 4 Storage moduli (G') and loss moduli (G'') obtained for SN hydrogels and DN hydrogels as a function of frequency.

decreased in the order of DN-0-10 > DN-10-0 > DN-3-7 > DN-7-3 > DN-5-5 and the order is similar to the change of the DN hydrogels' swelling ratio, indicating that the ratio of the first network to the second network determined the elasticity of the hydrogels.

Mechanical properties of hydrogels

The mechanical properties of the SN and DN hydrogels were measured by compressive test. The compressive stress–strain curves of these hydrogels were showed in Fig. 5a. The elastic modulus, maximum of compressive stress and strain of SN hydrogels was enhanced greatly by incorporating of a second PAAM polymer network. For instance, the elastic modulus of the DN-5-5 hydrogel is up to 5 times more than the according SN-5-5 hydrogel. The maxed compressive stress of the DN-7-3 increased from 0.0387 MPa to 0.4320 MPa, which is 11 times larger than the SN-7-3. The maxed compressive strain of the DN-3-7 is 3 times larger than the according SN-7-3. Therefore, the DN hydrogels showed improved mechanical performances.

Resistance to protein adsorption

Zwitterionic hydrogels are a class of excellent non-fouling materials. The protein absorption behaviors of the DN hydrogels were studied. BSA and LYZ, which have different isoelectric point (PI), were chosen as model protein to examine the non-fouling properties. As shown in Fig. 6, the amount of the protein adsorbed on these DN hydrogels has relation with the ratio of positively and negatively charged monomer and ionic strength. The negatively charged DN hydrogels and DN-5-5 showed excellent LYZ protein absorption resistance, whereas the DN-0-10 and DN-3-7 hydrogels showed much higher LYZ protein absorption (Fig. 6a). It is explained that positively charged LYZ could strongly adsorb on the negatively charged surfaces of the DN-0-10 and DN-3-7 hydrogels *via* electrostatic attraction interactions. Unexpectedly, all of the tested DN hydrogels exhibited relatively low adsorption of negative charged BSA protein (Fig. 6b).

Whitesides *et al.* studied the nonspecific protein adsorption of the betaine-type and the ampholyte-type self-assembled monolayers (SAMs) in different ionic strength, and pointed out that the amount of protein adsorbed on the ampholyte-type SAMs did not depend on the ionic strength.[46] Similar with this work, the protein adsorption of the equally mixed-charge DN-5-5 hydrogel is independent with ionic strength. In addition, the LYZ absorption amount in the DN-0-10 hydrogel increased with the ionic strength. However, the LYZ absorption amount in the DN-3-7 hydrogel initially increased and then decreased with the

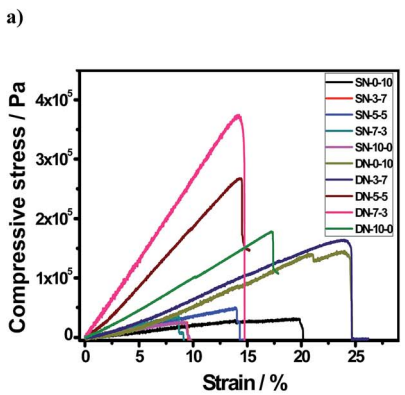

b)

Hydrogel No.	Elastic modulus/ MPa	Maxed compressive stress/MPa	Maxed compressive strain/%
SN-0-10	0.2172	0.0387	17.53
SN-3-7	0.4082	0.0296	6.90
SN-5-5	0.3768	0.0580	12.95
SN-7-3	0.4684	0.0387	8.30
SN-10-0	0.3231	0.0283	8.54
DN-0-10	0.4058	0.1849	21.31
DN-3-7	0.6141	0.2090	21.28
DN-5-5	2.0327	0.3089	13.46
DN-7-3	2.8842	0.4320	13.28
DN-10-0	1.0379	0.2120	15.82

Fig. 5 (a) Compressive stress–strain curves of the SN and DN hydrogels. (b) Elastic modulus, the maximum of compressive stress and strain obtained from compressive stress–strain curves. Elastic modulus values obtained from compressive stress–strain measurements calculated from the initial 5% strain.

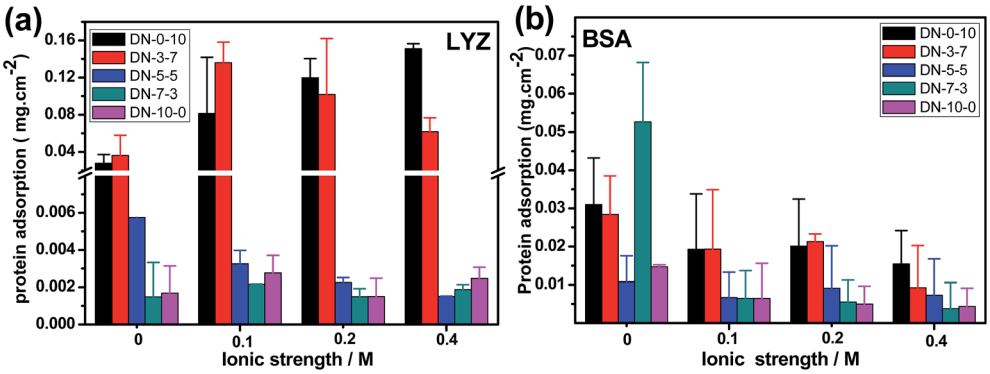

Fig. 6 Adsorption of LYZ (a) and BSA (b) on the DN hydrogel surfaces. The protein absorbed on the surface was washed out using a SDS solution. The concentration of the eluted protein solution was measured using a BCA protein determination method. The amount of the adsorbed proteins on the hydrogels was calculated according to the standard curves.

ionic strength. The LYZ absorption on the positively charged DN hydrogels such as DN-7-3 and DN-10-0 showed little relevance to the ionic strength. The BSA attachment amount on the DN hydrogels slightly decreased with the ionic strength.

Resistance to macrobiofouling: *Phaeodactylum tricornutum* and *Chlorella*

The settlement behaviors of *Chlorella* and *Phaeodactylum tricornutum* on the DN hydrogels' surfaces were studied (Fig. 7). After the *Chlorella* and *Phaeodactylum tricornutum* settlements for 1 day, the negatively charged DN-0-10, DN-3-7, and DN-5-5 samples showed better anti-algae performance than the positively charged DN-7-3 and DN-10-0 samples. After cultivation for 7 days, the *Chlorella* and *Phaeodactylum tricornutum* settlements on the surfaces of the DN-0-10 and DN-3-7 hydrogels reduced greatly but the amount on the surfaces of the DN-5-5, DN-7-3 and DN-10-0 samples increased. The anti-algae phenomenon on the negatively charged SA surface were also reported by Bauer.[47] The quantitative coverage areas of *Chlorella* and *Phaeodactylum tricornutum* on the hydrogels' surfaces were calculated according to the laser confocal images (Fig. 8b). The settlements of the *Chlorella* on the surfaces of the DN-0-10 and DN-3-7 hydrogels decreased approximately 40% and 80% after cultivation for 7 days, respectively. However, the coverage area on the surfaces of the DN-5-5, DN-7-3 and DN-10-0 hydrogels increased 2–6 times. The settlements of *Phaeodactylum tricornutum* on the DN hydrogels showed similar results. The optical photographs after cultivation for 7 days were shown in Fig. 8a. It can be seen that a large amount of *Phaeodactylum tricornutum* and *Chlorella* attached on the surfaces of the DN-5-5, DN-7-3 and DN-10-0 hydrogels but little algae were found on the surfaces of the DN-0-10 and DN-3-7 hydrogels. These results implied that the negative charged could efficiently

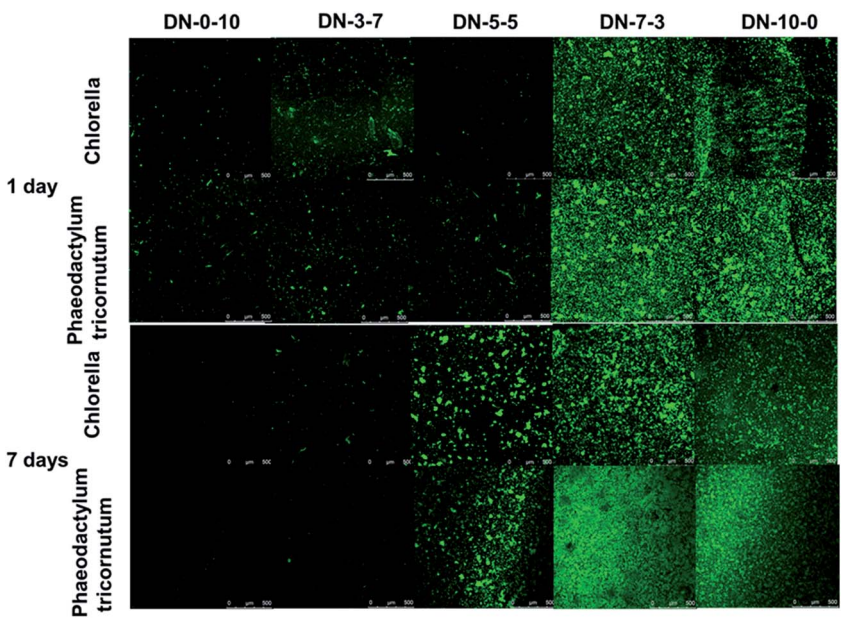

Fig. 7 Confocal images of *Chlorella* and *Phaeodactylum tricornutum* adhering onto the DN hydrogels after 1 day and 7 days.

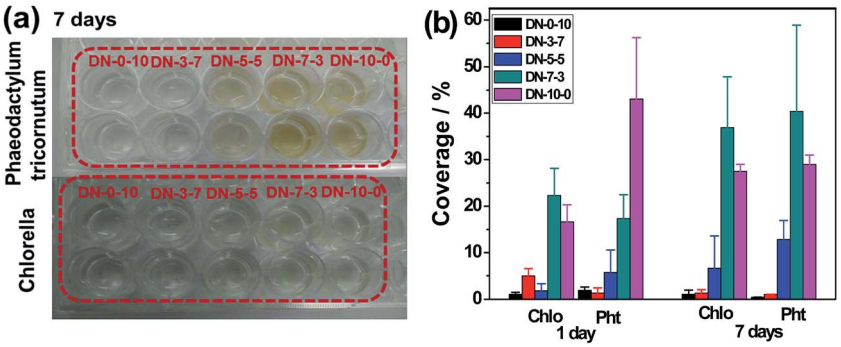

Fig. 8 (a) Photographs of *Phaeodactylum tricornutum* and *Chlorella* cultivated in a 24-well plate after 7 days. Each hydrogel was placed onto the bottom of the well; (b) quantitative coverage of Chlo and Pht on the hydrogels' surfaces. The quantitative coverage was calculated by software ImageJ based on the laser confocal images.

inhibit *Chlorella* and *Phaeodactylum tricornutum* by electrostatic repulsion of the negative surface of hydrogels and negative algaes.

Conclusions

The charged hydrogels were prepared by copolymerization of different ratios of TMA and SA. Then, the second PAAM network was incorporated to generate the DN hydrogels. Compared with the pristine SN hydrogels, the mechanical properties of the corresponding DN hydrogels were significantly improved. The amount of the protein absorbed on the hydrogels' surfaces greatly depended on the ratios of TMA/SA and the ionic strength. The DN hydrogels with a 1 : 1 ratio of TMA/SA exhibited excellent resistance of the protein adsorption. The anti-algae assay indicated that the negatively charged DN hydrogels showed better anti-algae performance than the positively charged and the 1 : 1 zwitterionic DN hydrogels. These excellent features of the DN hydrogels make them promisingly applied in marine antifouling materials.

Acknowledgements

The authors gratefully acknowledge financial support from the National Key Basic Research Program of China (2014CB643305), the National Nature Science Foundation (51303192), the Ningbo Major Special Project (2013B6012), the Youth Innovation Promotion Association Project (2015238), and the Innovative Team Projects of Zhejiang Province and Ningbo City (2011R50006; 2011B81001 and 2015B11003).

Notes and references

1 D. M. Yebra, S. Kiil and K. Dam-Johansen, *Prog. Org. Coat.*, 2004, **50**, 75–104.
2 M. P. Schultz, J. A. Bendick, E. R. Holm and W. M. Hertel, *Biofouling*, 2011, **27**, 87–98.
3 J. A. Callow and M. E. Callow, *Nat. Commun.*, 2011, **2**, 244–254.
4 A. A. Finnie and D. N. Williams, *Biofouling*, 2010, 185–206.
5 D. M. Yebra, S. Kiil and K. Dam-Johansen, *Prog. Org. Coat.*, 2004, **50**, 75–104.
6 A. Mukherjee, K. V. Monhan Rao and U. S. Ramesh, *J. Environ. Manage.*, 2009, **90**, 51–59.
7 N. Singh and A. Turner, *Mar. Pollut. Bull.*, 2009, **58**, 59–64.
8 R. A. King, J. D. A. Miller and J. S. Smith, *Br. Corros. J.*, 1973, **8**, 137–141.
9 R. A. King, *Nature*, 1971, **233**, 491–492.
10 S. Krishnan, A. Ramakrishnan, A. Hexemer, J. A. Finlay, K. E. Sohn, R. Perry, C. K. Ober, E. J. Kramer, M. E. Callow, J. A. Callow and D. A. Fischer, *Langmuir*, 2006, **22**, 5075–5086.
11 S. Krishnan, C. J. Weinman and C. K. Ober, *J. Mater. Chem.*, 2008, **18**, 3405–3413.
12 Y. J. Cho, H. S. Sundarm, C. J. Weinman, M. Y. Paik, M. D. Dimitriou, J. A. Finlay, M. E. Callow, J. A. Callow, E. J. Kramer and C. K. Ober, *Macromolecules*, 2011, **44**, 4783–4792.
13 Y. P. Wang, J. A. Finlay, D. E. Betts, T. J. Merkel, J. C. Luft, M. E. Callow, J. A. Callow and J. M. DeSimone, *Langmuir*, 2011, **27**, 10365–10369.
14 Z. Zhang, J. A. Finlay, L. Wang, Y. Gao, J. A. Callow, M. E. Callow and S. Y. Jiang, *Langmuir*, 2009, **25**, 13516–13521.
15 A. Kaffashi, A. Jannesari and Z. Ranjbar, *Biofouling*, 2012, **7**, 729–741.
16 S. B. Yeh, C. S. Chen, W. Y. Chen and C. J. Huang, *Langmuir*, 2014, **30**, 11386–11393.
17 S. M. Olsen, L. T. Pedersen, M. H. Laursen, S. Kiil and K. Dam-Johansen, *Biofouling*, 2007, **23**, 369–383.
18 N. Aldred, I. Y. Phang, S. L. Conlan, A. S. Clare and G. J. Vancso, *Biofouling*, 2008, **24**, 97–107.
19 X. J. Zhou, Z. Zhang, Y. Xu, C. L. Jin, H. P. He and X. J. Hao, *Biofouling*, 2009, **25**, 69–76.
20 D. Q. Feng, C. H. Ke, C. Y. Lu and S. J. Li, *Biofouling*, 2009, **25**, 181–190.
21 M. B. Angarano, R. F. McMahon, D. L. Hawkins and J. A. Schetz, *Biofouling*, 2007, **23**, 295–305.
22 A. S. Clare, *Biofouling*, 1996, **9**, 211–299.
23 T. Ekblad, G. Bergstroem, T. Ederth, S. L. Conlan, R. Mutton and A. S. Clare, *Biomacromolecules*, 2008, **9**, 2775–2783.

24 Y. Katsuyama, T. Kurokawa, T. Kaneko, J. P. Gong, Y. Osada and N. Yotsukura, *Macromol. Biosci.*, 2002, **2**, 163–169.
25 T. Murosaki, T. Noguchi, A. Kakugo, A. Putra, T. Kurokawa and H. Furukawa, *Biofouling*, 2009, **25**, 313–320.
26 T. Goda, R. Matsuno, T. Konno, M. Takai and K. Ishihara, *J. Biomed. Mater. Res., Part B*, 2009, **89**, 184–190.
27 L. R. Carr, Y. Zhou, J. E. Krause, H. Xue and S. Jiang, *Biomaterials*, 2011, **32**, 6893–6899.
28 J. M. Wang, H. Sun, J. J. Li, D. Y. Dong, Y. B. Zhang and F. L. Yao, *Carbohydr. Polym.*, 2015, **117**, 384–391.
29 Z. Zhang, T. Chao, L. Liu, G. Cheng, B. D. Ratner and S. Jiang, *J. Biomater. Sci., Polym. Ed.*, 2009, **20**, 1845–1859.
30 T. Ueda, H. Oshida, K. Kurita, K. Ishihara and N. Nakabayashi, *Polym. J.*, 1992, **24**, 1259.
31 S. Y. Jiang and Z. Q. Cao, *Adv. Mater.*, 2010, **22**, 920–932.
32 T. L. Sun, T. Kurokawa, S. Kuroda, A. B. Ihsan, T. Akasaki, K. Sato, M. A. Haque, T. Nakajima and J. P. Gong, *Nat. Mater.*, 2013, **12**, 932–937.
33 S. F. Chen and S. Y. Jiang, *Adv. Mater.*, 2008, **20**, 335.
34 M. A. Haque, T. Kurokawa and J. P. Gong, *Polymer*, 2012, **53**, 1805–1822.
35 Y. Okumura and K. Ito, *Adv. Mater.*, 2001, **13**, 485–487.
36 T. Sakai, T. Matsunaga, Y. Yamamoto, C. Ito, R. Yoshida, S. Suzuki, N. Sasaki, M. Shibayama and U. I. Chung, *Macromolecules*, 2008, **41**, 5379–5384.
37 K. J. Henderson, T. C. Zhou, K. J. Otim and K. R. Shull, *Macromolecules*, 2010, **43**, 6193–6201.
38 K. Haraguchi and T. Takehisa, *Adv. Mater.*, 2002, **14**, 1120–1124.
39 P. J. Schexnailder and G. Schmidt, *Colloid Polym. Sci.*, 2009, **287**, 1–11.
40 M. Shibayama, *Soft Matter*, 2012, **8**, 8030–8038.
41 P. Schexnailder, E. Loizou, L. Porcar, P. Butler and G. Schmidt, *Phys. Chem. Chem. Phys.*, 2009, **11**, 2760–2766.
42 H. Y. Yin, T. Akasaki, T. L. Sun, T. Nakajima, T. Kurokawa, T. Nonoyama, T. Taira, Y. Saruwatari and J. P. Gong, *J. Mater. Chem. B*, 2013, **1**, 3685–3693.
43 A. Venault, Y. S. Zheng, A. Chinnathambi, S. A. Alharbi, H. T. Ho, Y. Chang and Y. Chang, *Langmuir*, 2015, **31**, 2861–2869.
44 S. Liang, Q. M. Yu, H. Y. Yin, Z. L. Wu, T. Kurokawa and J. P. Gong, *Chem. Commun.*, 2009, 7518–7520.
45 A. B. Ihsan, T. L. Sun, S. Kuroda, M. A. Haque, T. Kurokawa, T. Nakajima and J. P. Gong, *J. Mater. Chem. B*, 2013, **1**, 4555–4562.
46 R. E. Holmlin, X. X. Chen, G. R. Chapman, S. Takayama and G. M. Whitesides, *Langmuir*, 2001, **17**, 2841–2850.
47 S. Bauer, M. Alles, J. A. Finlay, J. A. Callow, M. E. callow and A. Rosenhahn, *J. Biomater. Sci., Polym. Ed.*, 2014, **25**, 1530–1539.